C.P. No. 616

C.P. No. 616

MINISTRY OF AVIATION

AERONAUTICAL RESEARCH COUNCIL

CURRENT PAPERS

Comparative Thrust Measurements on a Series of Jet-flap Configurations and Circular Nozzles

by

M. N. Wood

LONDON: HER MAJESTY'S STATIONERY OFFICE

1962

PRICE 2s 9d NET

U.D.C. No. 533.694.6 : 533.697.4

C.P. No.616

January, 1962

COMPARATIVE THRUST MEASUREMENTS ON A SERIES OF JET-FLAP CONFIGURATIONS AND CIRCULAR NOZZLES

by

M. N. Wood

SUMMARY

Thrust measurements have been made with a range of jet-flap blowing configurations in an attempt to clarify the origins of the momentum losses associated with jet-flap wings. As a basis for comparison, thrust measurements have also been made on a series of simple circular nozzles. The relative importance of various factors which contribute to the losses has been determined, and ways of reducing the losses are suggested.

Previously issued as R.A.E. Tech. Note No. Aero. 2804 - A.R.C. 23,695.

LIST OF CONTENTS

LIST OF ILLUSTRATIONS

1 INTRODUCTION

With jet-flap wings, a large proportion of the efflux from the propulsive engines is ejected as a thin jet sheet over the upper surface of a trailing-edge flap. The latter is incorporated primarily to deflect the jet downwards through the required angle to the mainstream, with a resulting gain in pressure lift on the wing. It has been found that the jet loses an appreciable proportion of its momentum as it passes chordwise from the wing main duct to the flap trailing-edge, even when the flap is undeflected during cruise. Several factors contribute to this loss and an experiment was carried out on a half-model of an aspect-ratio 6 rectangular jet-flap wing to examine the relative importance of the various items. This necessitated extremely careful measurements of thrust and mass flow.

As a preliminary study, to establish a realistic and reliable basis for comparison, thrust measurements were made with a series of simple circular nozzles. Detailed velocity traverses were also made across the exits of these nozzles in an attempt to estimate the rate at which momentum was being ejected.

2 MODEL DETAILS AND EXPERIMENTAL METHOD

Three different sharp-edged circular nozzles, designated A, B and C in Fig.2, were made with an exit diameter of 2·000 inches and a contraction ratio of 9:1. On nozzle A the interior and exterior shapes were simple cones of 8·75° and 14° semi-angle respectively. The exterior of nozzle B was identical with that of A, but the inside contour consisted of a 16° cone followed by 6 inches of constant section. The contraction of nozzle C was identical with B, but the exterior contour was concave and so shaped that, over the last 2 inches of the nozzle, the wall thickness was less than 0·02 inches, being sharp-edged at the exit. Annular collars were made to fit round nozzles A and B so as to produce a bluff exit face of up to 6 inches external diameter. The nozzles were mounted on a section of standard 6 inch steel pipe.

The basic jet-flap model comprised the rectangular half wing and body used in earlier jet-flap experiments. (Refs. 1,2). The wing was a symmetrical 12% thick modified R.A.E. 104 section and the chord varied between 18·8 and 20 inches depending on the trailing-edge condition. Details of the various jet-flap configurations tested are given in Fig.1. The blowing nozzle consisted of a gentle contraction followed by a parallel slot section which was five slot widths in length. In all conditions, the nominal slot width was 0·08 inches, though in practice it varied between 0·079 and 0·085 inches. The slot width variation over the 54 inch slot span was carefully measured over the range of pressure ratio, so that the slot exit area was known to within about ±1%. In the flap blowing configurations the slot width was set with 0·115 inch wide rectangular spacers every two inches across the span. Full-span flaps of one and two inch chord were available and the hinge point could be moved normal to the wing lower surface. In the trailing-edge blowing configuration, the gap was fixed by spacers in the contraction, so that spacers in the slot itself were unnecessary. Tests were first made without slot spacers and then with 0·25 inch and 0·5 inch wide rectangular spacers, at two inch intervals across the span. The basic trailing-edge thickness was 0.34 inches. This bluffness could be increased to 0·9 inch with the additional trailing-edge pieces shown in Fig.1. Simple full-span, 1 inch and 2 inch long, flat plate chord extensions were tested with the trailing-edge blowing, the upper surface being taken as a continuation of the lower slot wall, thus representing a flap with zero deflection angle.

The thrust measurements were made with the models mounted on the under floor balance of the No.2 11½ ft × 8½ ft tunnel at R.A.E. and in all cases the compressed air jets were ejected into the working section of the tunnel. The circular nozzles were tested only at zero tunnel speed with blowing pressure ratios between 1·07 and 1·85. For the jet-flap wing, the maximum available pressure ratio was 1·5 with no slot spacers, and 2·1 with maximum blockage; the tunnel speed was varied between 0 and 250 ft/sec. Care was taken with all the static thrust measurements to check the interference from the tunnel walls and from the flow induced round the tunnel. With the circular nozzles, the jets were directed upstream into the maximum section of the tunnel to minimise flow recirculation and, by shielding the 6 inch pipe and flanges, it was checked that there were no induced thrust losses, except for possible boundary-layer losses on the external surfaces of the actual nozzles.

The measurements of mass-flow rate, Q, were taken outside the tunnel on a static calibrating rig, using a standard orifice plate of area-ratio 0·5 (Ref. 3 Ch.6), in the 6 inch pipeline ahead of the jet. The mass-flow was calibrated against a reference pressure upstream of the jet which was simply related to the mean total head p_D in the jet outside the nozzle wall boundary-layer. A theoretical isentropic mass flow Q_1 was calculated using p_D, atmospheric pressure p_o, duct stagnation temperature T_D and the jet exit area. (See Appendix.) In general Q_1 is slightly larger than Q, since the estimate of Q_1 ignores the boundary-layer losses. With the circular nozzles, traverses of total pressure p_t, and static pressure p_s were made across the jet face, in order to estimate these losses. The total head tube had an external diameter of 0·020 inches, and corrections were made for wall and boundary-layer interference, using Ref.4. The static tube was 0·12 inches in diameter and was of a shape to give zero correction when used in a uniform stream. There was a possible error in the present case, as only a short length of the supporting stem was in the jet stream. However, the static pressure traverses agreed well with inner wall static pressure measurements near the exit of nozzle B, so the error was assumed to be negligible. From p_s, p_t and T_D, it was possible to calculate the local mean value of ρV, and hence to derive a second estimate of mass flow

$$Q_2 = \int 2\pi r \rho V \, dr = \int_0^1 \frac{2\pi r}{144} \frac{108{\cdot}31}{\sqrt{T_D}} \left\{ 1 - \left(\frac{p_s}{p_t}\right)^{\frac{2}{7}} \right\}^{\frac{1}{2}} \left(\frac{p_t}{p_s}\right)^{\frac{2}{7}} p_s \, dr \quad .$$

It was assumed that the ratios $\frac{Q}{Q_1}$, $\frac{Q_2}{Q_1}$ were functions only of the nozzle geometry and $\frac{p_D}{p_o}$, and that they were independent of day-to-day variations in p_o, T. This assumption was quite reasonable and was necessitated by the fact that, with the existing rig, mass flow Q could not be measured directly when the model was mounted on the balance.

A purely theoretical estimate M_1 of the jet momentum was derived assuming constant total and static pressure p_D, p_o across the jet. (See Appendix.) A second semi-theoretical estimate $Q V_j$, was obtained using

the theoretical centre-line exit velocity V_j obtained by isentropic expansion from p_D to p_o; this is the usual reference momentum quoted for jet flap model results. For the circular nozzles a further estimate M_2 was obtained by integrating across the jet face the product of the local value of ρV and the theoretical V', assuming isentropic expansion from local p_t to p_o.

$$M_2 = \int_o^1 \frac{2\pi r}{144} \times 495{\cdot}0\ p_s \left\{1 - \left(\frac{p_s}{p_t}\right)^{\frac{2}{7}}\right\}^{\frac{1}{2}} \left\{1 - \left(\frac{p_o}{p_t}\right)^{\frac{2}{7}}\right\}^{\frac{1}{2}} \left(\frac{p_t}{p_s}\right)^{\frac{2}{7}} dr \quad .$$

Once again the ratios $\frac{Q\ V_j}{M_1}$, $\frac{M_2}{M_1}$ were assumed to be independent of day-to-day variations in atmospheric pressure.

Slot boundary-layer traverses were not attempted with the jet flap wing, but the spanwise variation of centre-line total pressure was carefully measured to give a mean value for p_D. From this and the measured mass flow, the quantities Q_1, M_1 and $Q\ V_j$ could be calculated. The ratio $\frac{Q}{Q_1}$ could be used as a rough guide of the slot boundary-layer thickness in conditions where there was approximately atmospheric pressure p_o at the exit (see section 4.1). Hence, on the assumption of a specific boundary-layer profile in the slot, a quantity M_2 could be defined equivalent to the M_2 for the circular nozzles.

3 CIRCULAR NOZZLE RESULTS

The mass flow calibration revealed that the ratio $\frac{Q}{Q_1}$ was virtually constant for nozzles B and C rising from 0·965 at a pressure-ratio of 1·1 to 0·97 when $\frac{p_D}{p_o}$ was 1·85. For the convergent nozzle A, $\frac{Q}{Q_1}$ increased linearly with pressure-ratio, the results giving a relationship $\frac{Q}{Q_1} = 0{\cdot}945 + 0{\cdot}05\left(\frac{p_D}{p_o} - 1\right)$. The additional bluffness of the 6 inch diameter annular ring had no noticeable effect on the calibration.

Traverses of total pressure p_t were made at pressure ratios of 1·33 and 1·85 along several different radii across the face of each nozzle. These showed that the boundary-layer growth was, for all practical purposes, symmetrical round the jet circumference. Fig.4 shows the boundary-layer profiles for the two different contraction shapes; local velocity V' has been calculated from p_t and p_o.

Static pressure traverses were done in less detail. With the parallel nozzles B and C, the pressure was atmospheric across the jet, within the accuracy of the measurements. However, there was a large pressure gradient across the face of nozzle A as shown in Fig.3.

For the parallel nozzles B and C the ratio $\frac{Q}{Q_2}$, which should be unity, was 1·002 at $\frac{p_D}{p_o} = 1{\cdot}33$ and 1·008 at $\frac{p_D}{p_o} = 1{\cdot}85$ so that agreement was very good.

For the contracting nozzle, where the estimates of Q_2 and M_2 were more dependent on the accuracy of the static pressure traverses the corresponding ratios were 1·010 and 1·008 respectively.

The thrust M_T was measured on the balance over a range of pressure ratios $\frac{p_D}{p_o}$ from 1·25 to 1·85. For the parallel nozzles, the ratios $\frac{M}{M_2}$. $\frac{M}{Q\ V_j}$ and $\frac{M}{M_1}$ were 1·00, 0·97 and 0·94 respectively. Possible inaccuracies in the various measurements of pressure, mass flow and thrust should not give more than about ±1% error in these values. There was no measurable difference between results with nozzle C of zero bluffness and nozzle B with the 6 inch diameter annular collar. For the contracting nozzle A, the ratios $\frac{M}{M_2}$, $\frac{M}{Q\ V_j}$ were 1·005 and 0·990 respectively, showing that the thrust was equal to M_2, defined in section 2 as $\int_0^1 2\pi\ r\ \rho\ V\ V'\ dr$. On the other hand, the actual momentum, $\int_0^1 2\pi\ r\ \rho\ V^2\ dr$ at the exit of nozzle A was considerably less than M_2, due to the large static pressure at the exit, being only about 80% at the pressure-ratio of 1·85.

These tests on the circular nozzles confirmed the reliability of the orifice plate for measurements of mass flow, and showed, for the circular nozzles at least, that the thrust generated was equal to the momentum produced on the assumption that the air expanded isentropically to atmospheric pressure.

4 JET FLAP RESULTS

4.1 Static tests

The mass flow Q was calibrated against internal duct pressure over the range of configurations for which the thrust was measured. The results are summarised in Fig.5, where the ratio $\frac{Q}{Q_1}$ is plotted against pressure-ratio $\frac{p_D}{p_o}$. The datum position for the flap blowing was with the flap upper surface approximately tangential to the upper edge of the jet. This generated a back pressure in the slot due to the impact of the jet on the flap and reduced the mass flow by as much as 4 per cent. In contrast, with the trailing-edge blowing slot, additional bluffness increased the suction at the exit giving a rise in mass flow.

The thrusts could most readily be discussed in terms of the known $Q\ V_j$ values, as M_2 could not be estimated directly due to the fact that no boundary-layer traverses were attempted. It was only possible to infer the boundary-layer thickness from an examination of values for $\frac{Q}{Q_1}$ obtained when

the jet exit static pressure was atmospheric, and hence, by assuming a specific boundary-layer profile, to obtain rough estimates of $\frac{M_2}{M_1}$ and $\frac{M_2}{Q\ V_j}$. It would appear that the ratio $\frac{M_2}{Q\ V_j}$ probably lay between 0·95 and 0·97, and this would not conflict with rough theoretical estimates of boundary-layer growth inside the slot.

With trailing-edge blowing and with no slot blockage the ratio $\frac{M_T}{Q\ V_j}$ was constant at 0·945, independent of pressure-ratio. Removal of the fuselage showed that ½% to 1% of the momentum was lost through skin friction on the rear fuselage. Thus, without the fuselage, the ratio $\frac{M_T}{M_2}$ would be expected to lie between 0·98 and 1·00. Any remaining loss was probably due to the suction on the slightly bluff trailing-edge in the basic case. Increasing the bluffness to 0·9 inches produced a further 3% loss.

When the simple full-span, flat plate chord extensions were fitted, representing undeflected flaps, $\frac{M_T}{Q\ V_j}$ fell from 0·945, the basic value, to 0·91 and 0·89, for the 1 inch and 2 inch chord extensions respectively.

With the largest span spacers (0·5 inch wide) fitted at 2 inch intervals along the slot, a large variation of $\frac{Q}{Q_1}$ with pressure-ratio was introduced, (see Fig.5) but no explanation could be offered. The ratio $\frac{M_T}{Q\ V_j}$ was 0·93 and 0·925 with spacer widths of 0·25 inch and 0·5 inch as against the basic value of 0·945. It seems unlikely that the ratio $\frac{M_2}{Q\ V_j}$ would remain constant when spacers were fitted.

For the flap-blowing configurations proper, it was found that the optimum position for the flap was with its upper surface approximately tangential to the lower jet boundary. For example, $\frac{M_T}{Q\ V_j}$ was 0·835 with the 2 inch chord flap in the datum position, with the flap tangential to the upper jet boundary. The ratio increased as the flap was lowered, reaching a maximum value of 0·865 with the flap 0·10 inches below the datum, and then falling away again, reaching 0·835 at a depth of 0·25 inches below datum. The difference between this maximum value of 0·865 and the value of 0·89 recorded with the trailing-edge blowing slot and 2 inch chord extension was due partly to the presence of spacers in the true flap-blowing slot, and partly perhaps to the more gentle contraction (see Fig.1) which could be expected to give a thicker boundary-layer.

Lowering the flap produced a small gap between the flap and the main wing, and the above results were obtained with this gap sealed. With the flap in the optimum position, the gap size was about half the slot width, and it was found that a gain of about 1% in $\frac{M_T}{Q\ V_j}$ could be achieved by unsealing the gap. The gap size did not appear to be very critical, as similar thrust increments were obtained with all other flap positions except for those where impact of the jet on the flap produced a high

pressure at the jet exit, as in the datum case. This effect was most probably due to air drawn from the wing lower surface, producing a buffer between the flap and the jet and thus reducing the flap skin friction losses.

4.2 Effects of forward speed

At forward speed, the momentum M_T has been taken as the sum of the measured thrust, the basic wing drag with no jet flow, and the estimated lift-dependent drag[5], which was always small. With the 2 inch chord flap in the datum position, the upper and lower wing surfaces were almost continuous to the sharp trailing-edge and the basic wing drag was then a minimum. In this condition, forward speed had no effect on $\frac{M_T}{Q\ V_j}$, which was constant at 0·835 over the range of velocity ratio $\frac{V_o}{V_j}$ from 0 to 0·5. Dropping the flap 0·1 inches had little effect on the basic wing drag, in spite of slight steps in the wing contour, and again forward speed had no effect on $\frac{M_T}{Q\ V_j}$.

In the other conditions, steps in the contour, or trailing-edge bluffness, were sufficient to cause a significant increase in basic wing drag, due partly to the suction on the rearward faces. Suction was also generated on these faces by jet flow at zero forward speed and when the two effects were combined, the results were difficult to understand. Forward speed decreased the value of $\frac{M_T}{Q\ V_j}$ and the effect became more marked as the bluffness increased. In the worst condition, with the 0·9 inch thick trailing-edge and a forward speed of 250 ft/sec, $\frac{M_T}{Q\ V_j}$ was reduced to about 92% of the static value. The results were not conclusive, but the decrease appeared to be dependent on velocity, rather than velocity-ratio as would have been expected.

4.3 Effect of flap angle

A few measurements of resultant force were made at zero nominal tunnel speed for flap angles of 30°, 60° and 90°. In these conditions the velocities induced round the tunnel and the interference from the tunnel walls, could have a significant effect on the measurements. Though attempts were made to assess the overall interference, the results should be treated with caution. It appeared that the ratio between the resultant force and the zero flap angle thrust was approximately 1·00, 0·96, 0·81 at flap angles of 30°, 60° and 90° respectively, so that large deflections of the jet could be achieved with quite small turning losses. It was not known to what extent the results depended on the particular flap geometry tested.

At forward speed, with the flaps deflected, the lift-dependent drag is larger than would be estimated by existing theory. This problem has been discussed elsewhere[5], but unfortunately, in the absence of reliable force measurements on 2-dimensional blowing configurations, no satisfactory form of analysis is available.

5 CONCLUSIONS

The results have shown that there are two main sources of momentum loss with jet-flap wings at small deflection angles, namely boundary-layer growth in the blowing slot, and skin friction losses over the upper surface of the

trailing-edge flap normally used to produce the jet deflection. With careful design of the slot geometry, to avoid separation and to minimise skin friction, there is no reason why the boundary-layer losses should exceed those for simple circular nozzles. If a trailing-edge flap is used there will certainly be a further loss, but this can be reduced to perhaps 3% or 4% by keeping the flap as small as possible compatible with high lift requirements, and by careful alignment of the flap relative to the blowing slot. Of course, if the flap is not needed except for high lift and can be retracted without leaving excessive trailing-edge bluffness, this loss will not affect the cruise performance.

LIST OF SYMBOLS

p_D duct total pressure

p_o atmospheric or free stream static pressure

p_t local total pressure

p_s local static pressure

ρ local density

T local temperature in °C

T_D duct temperature in °C

V local velocity $= 147{\cdot}1 \sqrt{T_D \left(1 - \left(\frac{p_s}{p_t}\right)^{\frac{2}{7}}\right)}$ ft/sec

V' theoretical, expanded local velocity $= 147{\cdot}1 \sqrt{T_D \left(1 - \left(\frac{p_o}{p_t}\right)^{\frac{2}{7}}\right)}$

V_j theoretical, expanded centre-line velocity $= 147{\cdot}1 \sqrt{T_D \left(1 - \left(\frac{p_o}{p_D}\right)^{\frac{2}{7}}\right)}$

Q measured mass flow

Q_1 mass flow estimate based on V_j and area

Q_2 mass flow estimate $= \int \rho \, V \, dS$

M_T measured thrust or momentum

M_1 momentum estimate based on V_j and area

M_2 momentum estimate $= \int \rho \, V \, V' \, dS$

LIST OF REFERENCES

No.	Author	Title, etc.
1	Alexander, A.J., Williams, J.	Wind-tunnel experiments on a rectangular-wing jet-flap model of aspect-ratio 6. A.R.C. 22,947. June, 1961.
2	Wood, M. N.	Further wind tunnel experiments on a rectangular-wing jet-flap model of aspect-ratio 6. Unpublished M.O.A. Report.
3	Ower, E.	The measurement of air flow (2nd Edition)
4	MacMillan, F.A.	Experiments on pitot tubes in shear flow. A.R.C. R. & M. 3028. February, 1956.
5	Williams, J., Butler, S.F.J., Wood, M.N.	The aerodynamics of jet flaps. A.R.C. R. & M. 3304. January, 1961.

APPENDIX

Bernoulli's equation for compressible flow gives

$$\frac{p_D}{\rho_D} = \frac{p}{\rho} + \frac{\gamma-1}{2\gamma} V^2$$

where p_D, ρ_D are stagnation pressure and density respectively, and p, ρ are ambient conditions where the local velocity is V. γ is the ratio of the specific heats.

For isentropic processes $\frac{p}{\rho^\gamma}$ = const from which

$$\frac{p}{\rho} = \frac{p_D}{\rho_D}\left(\frac{p}{p_D}\right)^{\frac{\gamma-1}{\gamma}} .$$

The speed of sound $a = \sqrt{\gamma \frac{p}{\rho}} = \sqrt{\gamma R T}$ where T is the local temperature and R is the gas constant.

Hence

$$V^2 = a_D^2 \frac{2}{\gamma-1}\left\{1 - \left(\frac{p}{p_D}\right)^{\frac{\gamma-1}{\gamma}}\right\}$$

giving

$$V = 147{\cdot}1 \sqrt{T_D}\left\{1 - \left(\frac{p}{p_D}\right)^{\frac{2}{7}}\right\}^{\frac{1}{2}} \text{ ft/sec}$$

where the duct stagnation temperature T_D is in ^{o}Kelvin and $\gamma = 1{\cdot}4$.

Now

$$\rho = p\frac{\rho_D}{p_D}\left(\frac{p_D}{p}\right)^{\frac{\gamma-1}{\gamma}} = \frac{p}{R\,T_D}\left(\frac{p_D}{p}\right)^{\frac{\gamma-1}{\gamma}}$$

therefore

$$\rho V = \frac{108{\cdot}3}{\sqrt{T_D}} \left\{ 1 - \left(\frac{p}{p_D}\right)^{\frac{2}{7}} \right\}^{\frac{1}{2}} \left(\frac{p_D}{p}\right)^{\frac{2}{7}} p \text{ lb/sq ft/sec}$$

where the local pressure p is measured in inches of mercury. Hence the mass flow can be determined for the circular nozzles and in the notation of the main text

$$Q_1 = \int_0^1 \frac{2\pi r}{144} \frac{108{\cdot}3}{\sqrt{T_D}} \left\{ 1 - \left(\frac{p_o}{p_D}\right)^{\frac{2}{7}} \right\}^{\frac{1}{2}} \left(\frac{p_D}{p_o}\right)^{\frac{2}{7}} p_o \, dr \text{ lb/sec}$$

and

$$Q_2 = \int_0^1 \frac{2\pi r}{144} \frac{108{\cdot}3}{\sqrt{T_D}} \left\{ 1 - \left(\frac{p_s}{p_t}\right)^{\frac{2}{7}} \right\}^{\frac{1}{2}} \left(\frac{p_t}{p_s}\right)^{\frac{2}{7}} p_s \, dr \text{ lb/sec}$$

with r measured in inches.

In producing the first estimate of momentum M_1 $(= Q_1 V_j)$ the pressures p_D, p_o have been used to define ρ and V_j giving

$$\rho V_j^2 = \frac{p}{R T_D} \left(\frac{p_D}{p_o}\right)^{\frac{\gamma-1}{\gamma}} \frac{2a_D^2}{\gamma-1} \left(1 - \left(\frac{p_o}{p_D}\right)^{\frac{\gamma-1}{\gamma}}\right)$$

$$= \frac{2\gamma p_o}{\gamma-1} \left\{ \left(\frac{p_D}{p_o}\right)^{\frac{\gamma-1}{\gamma}} - 1 \right\}$$

and hence

$$M_1 = \int_0^1 \frac{2\pi r}{144} 495{\cdot}0 \, p_o \left\{ \left(\frac{p_D}{p_o}\right)^{\frac{2}{7}} - 1 \right\} dr \text{ lb wt}$$

where p_o is in inches of mercury.

In determining M_2 the pressures p_t, p_s have been used to define the mass flow rate ρV, but the effective velocity V' for the momentum has been obtained by assuming isentropic expansion from local stagnation pressure p_t to atmospheric pressure p_o. Hence

$$M_2 = \int 2 \pi r \rho V V' \, dr$$

$$= \int_0^1 \frac{2\pi r}{144} 495{\cdot}0 \, p_s \left\{ 1 - \left(\frac{p_s}{p_t}\right)^{\frac{2}{7}} \right\}^{\frac{1}{2}} \left\{ 1 - \left(\frac{p_o}{p_t}\right)^{\frac{2}{7}} \right\}^{\frac{1}{2}} \left(\frac{p_t}{p_s}\right)^{\frac{2}{7}} dr \, .$$

WT.2078.C.P.616.K3 - Printed in England

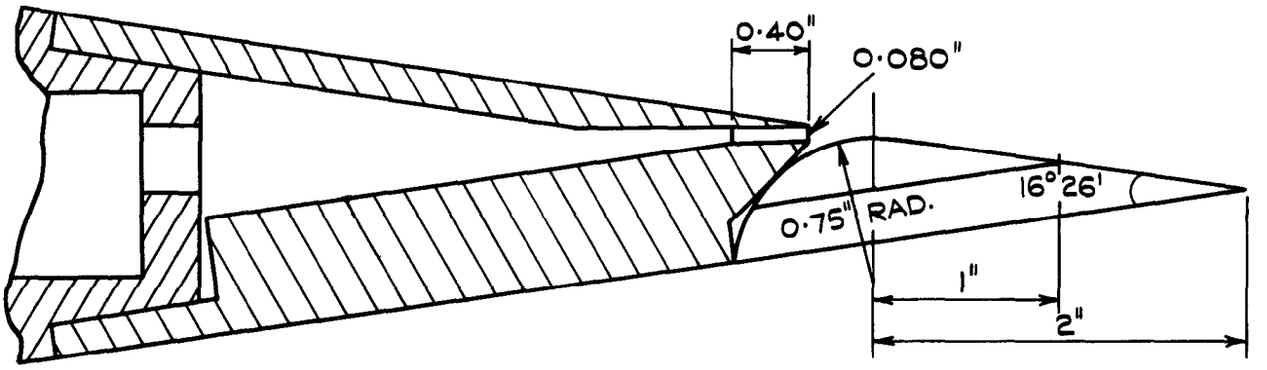

FLAP BLOWING

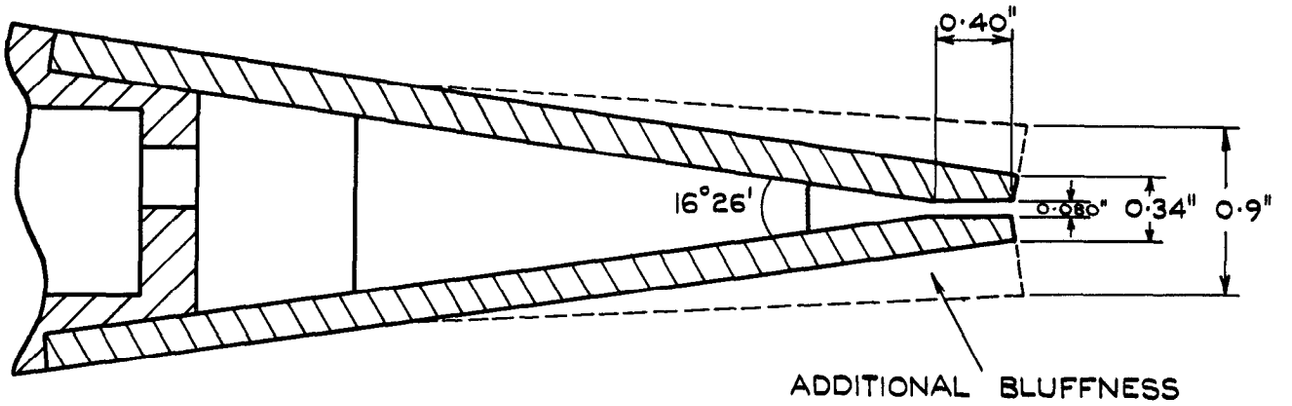

TRAILING EDGE BLOWING

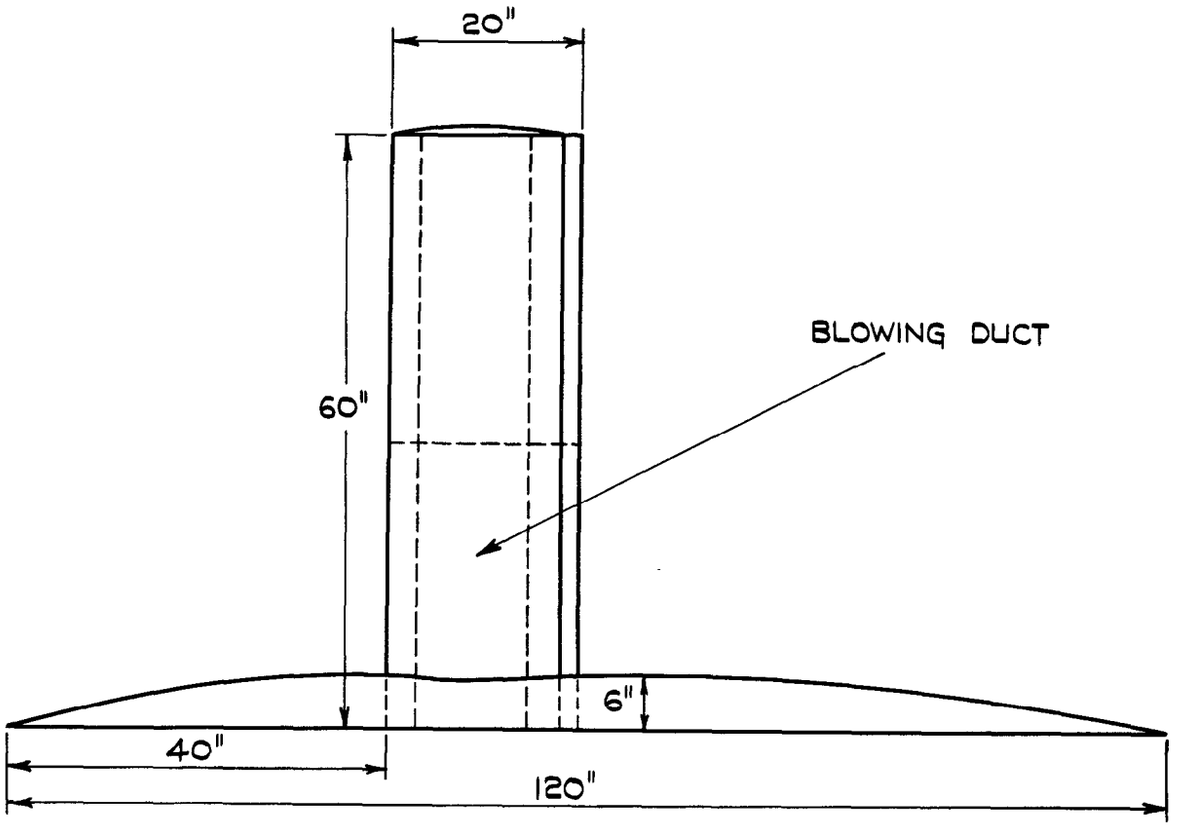

FIG. 1. HALF-MODEL JET FLAP CONFIGURATIONS.

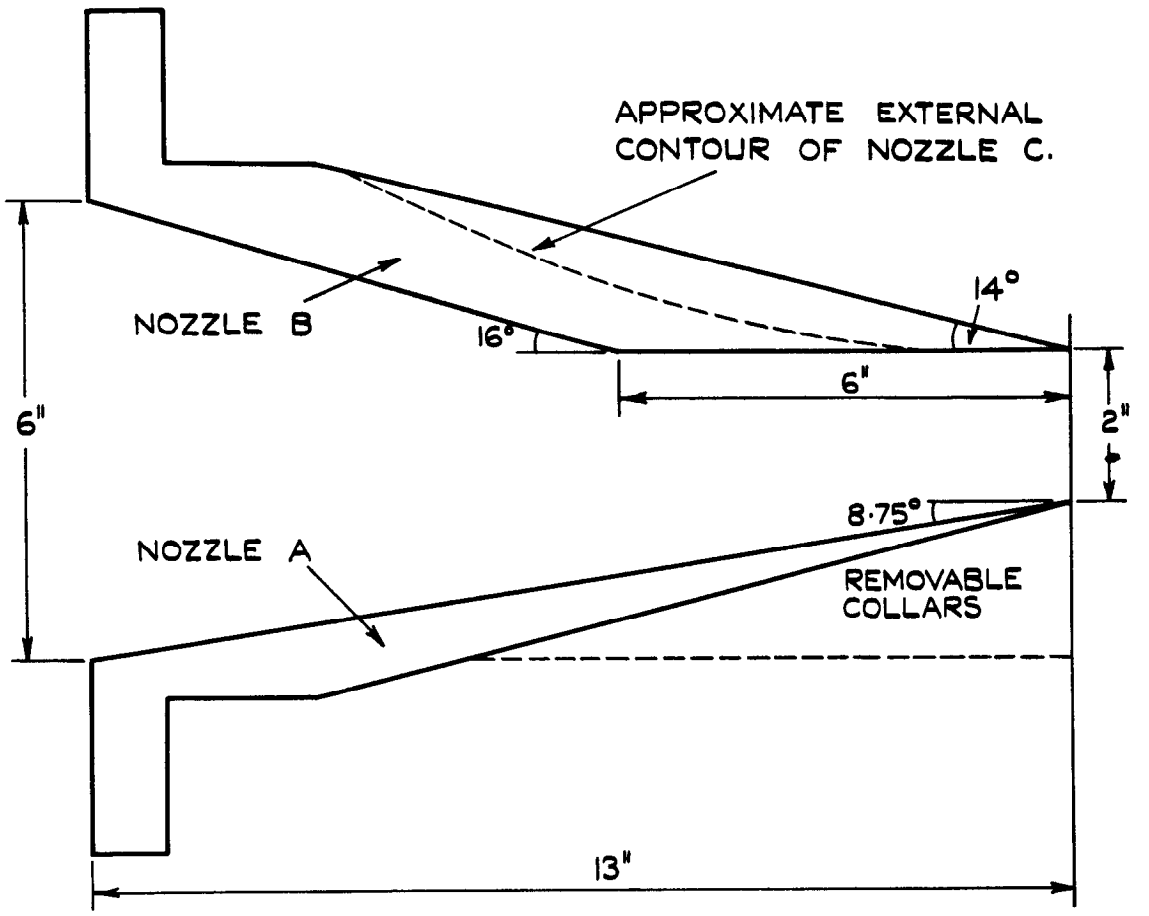

FIG. 2. DETAILS OF CIRCULAR NOZZLES.

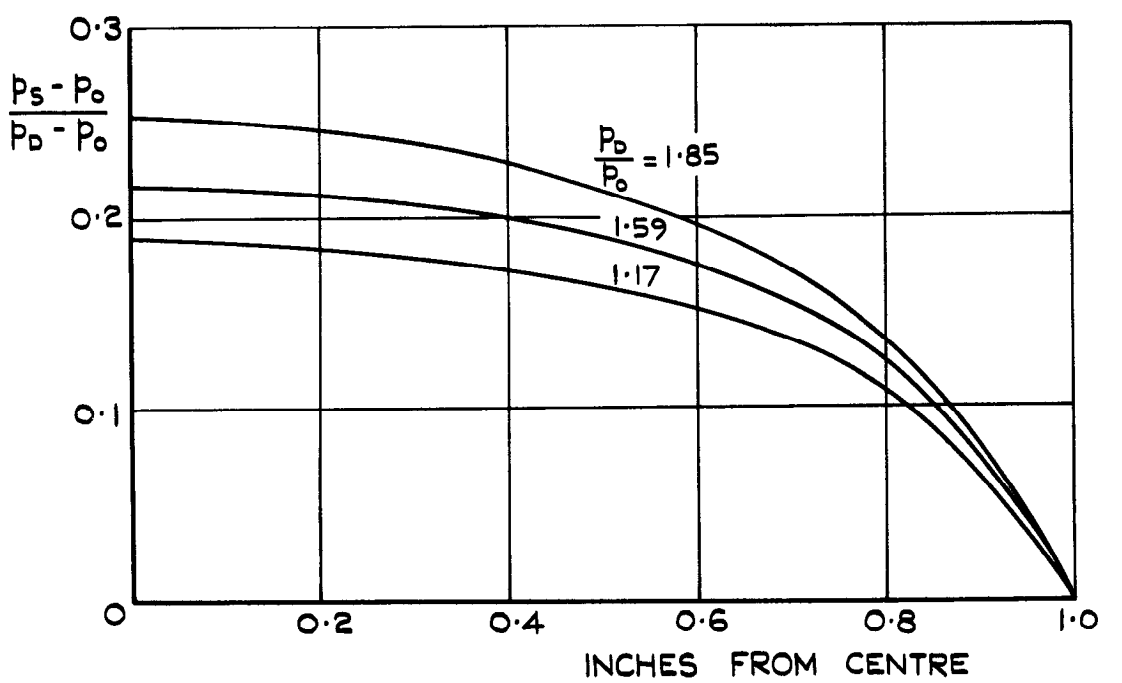

FIG. 3. STATIC PRESSURE DISTRIBUTION.
NOZZLE A.

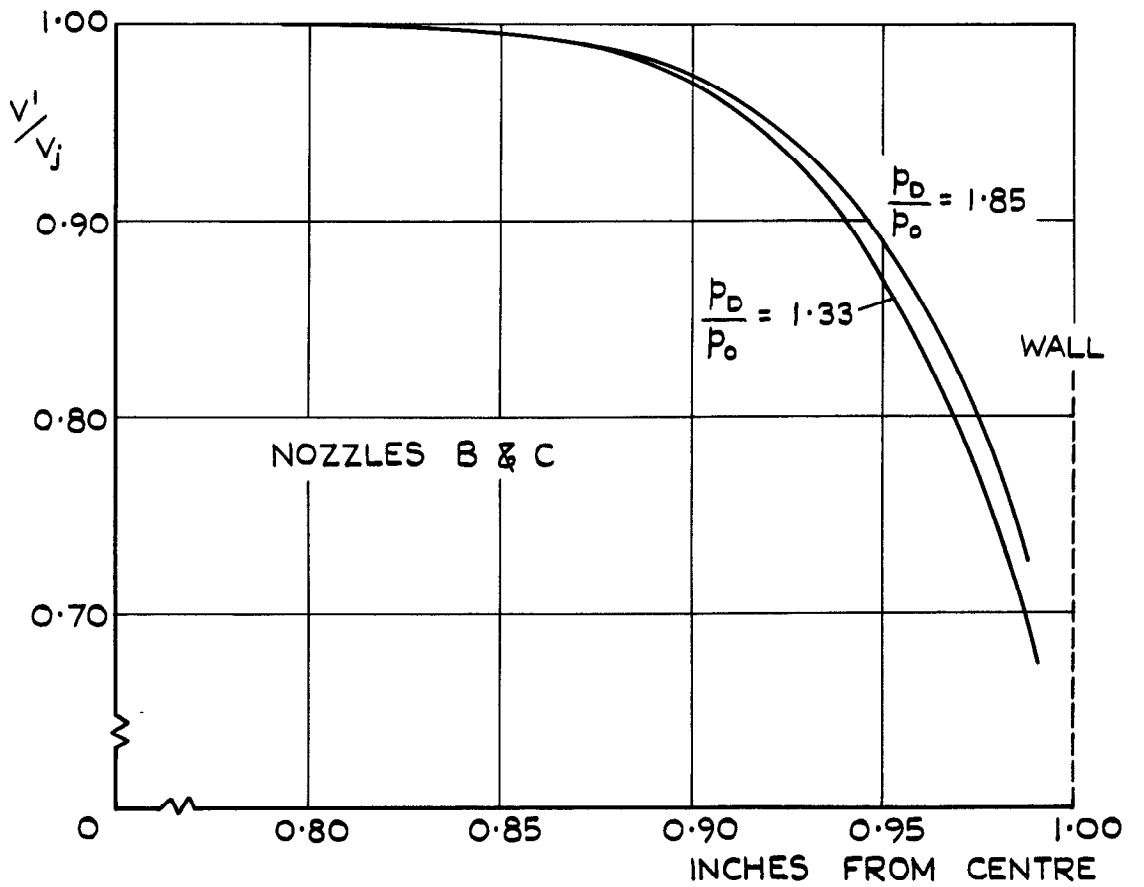

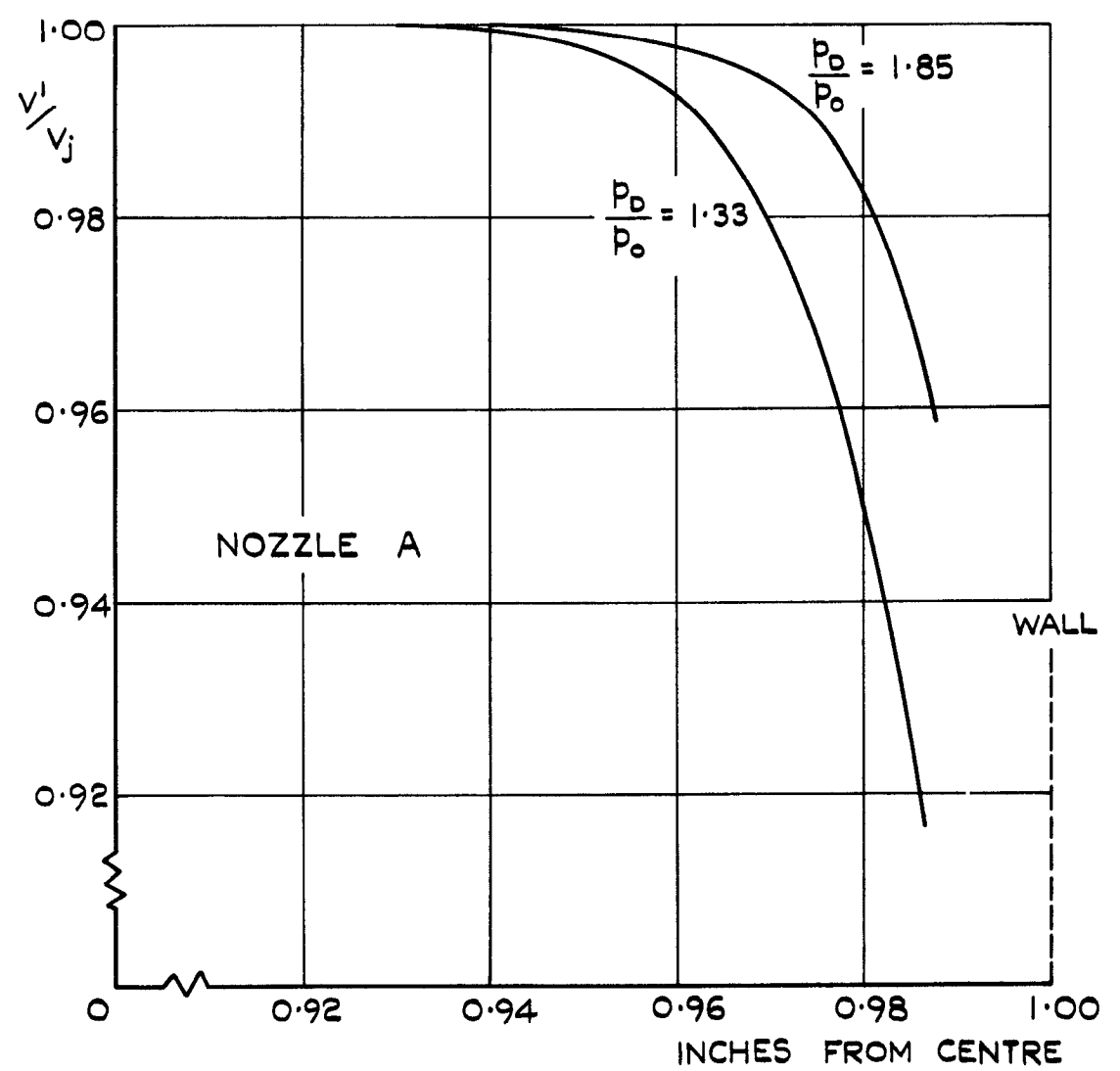

FIG. 4. BOUNDARY-LAYER GROWTH INSIDE CIRCULAR NOZZLES.

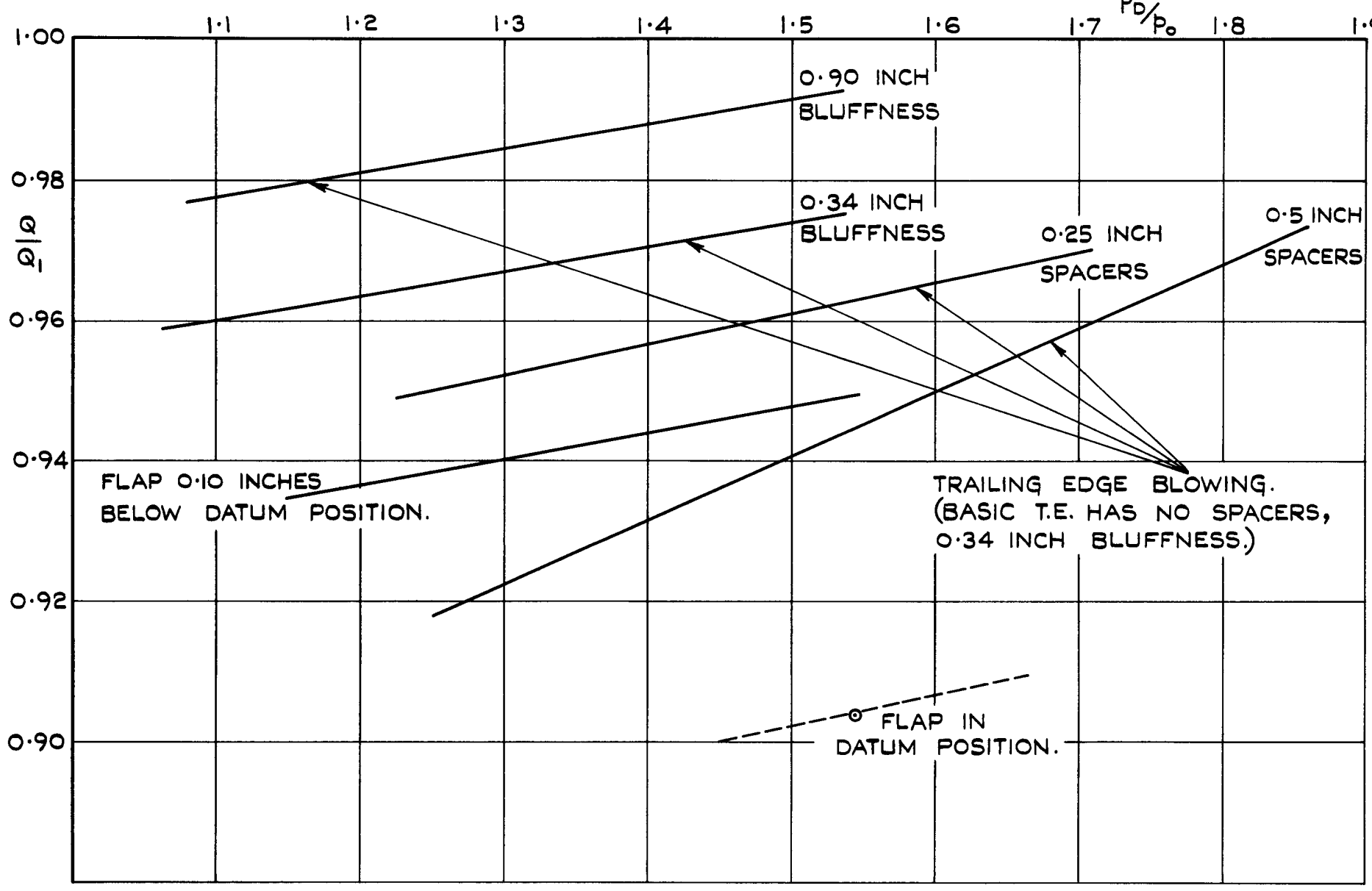

FIG. 5. JET - FLAP MASS FLOW CALIBRATION.

A.R.C. C.P. No.616

533.694.6 :
533.697.4

COMPARATIVE THRUST MEASUREMENTS ON A SERIES OF JET-FLAP CONFIGURATIONS AND CIRCULAR NOZZLES.. Wood, M.N.
January, 1962.

Thrust measurements have been made with a range of jet-flap blowing configurations in an attempt to clarify the origins of the momentum losses associated with jet-flap wings. As a basis for comparison, thrust measurements have also been made on a series of simple circular nozzles. The relative importance of various factors which contribute to the losses has been determined, and ways of reducing the losses are suggested.

A.R.C. C.P. No.616

533.694.6 :
533.697.4

COMPARATIVE THRUST MEASUREMENTS ON A SERIES OF JET-FLAP CONFIGURATIONS AND CIRCULAR NOZZLES. Wood, M.N.
January, 1962.

Thrust measurements have been made with a range of jet-flap blowing configurations in an attempt to clarify the origins of the momentum losses associated with jet-flap wings. As a basis for comparison, thrust measurements have also been made on a series of simple circular nozzles. The relative importance of various factors which contribute to the losses has been determined, and ways of reducing the losses are suggested.

A.R.C. C.P. No.616

533.694.6 :
533.697.4

COMPARATIVE THRUST MEASUREMENTS ON A SERIES OF JET-FLAP CONFIGURATIONS AND CIRCULAR NOZZLES. Wood, M.N.
January, 1962.

Thrust measurements have been made with a range of jet-flap blowing configurations in an attempt to clarify the origins of the momentum losses associated with jet-flap wings. As a basis for comparison, thrust measurements have also been made on a series of simple circular nozzles. The relative importance of various factors which contribute to the losses has been determined, and ways of reducing the losses are suggested.

A.R.C. C.P. No.616

533.694.6 :
533.697.4

COMPARATIVE THRUST MEASUREMENTS ON A SERIES OF JET-FLAP CONFIGURATIONS AND CIRCULAR NOZZLES. Wood, M.N.
January, 1962.

Thrust measurements have been made with a range of jet-flap blowing configurations in an attempt to clarify the origins of the momentum losses associated with jet-flap wings. As a basis for comparison, thrust measurements have also been made on a series of simple circular nozzles. The relative importance of various factors which contribute to the losses has been determined, and ways of reducing the losses are suggested.

Published by
HER MAJESTY'S STATIONERY OFFICE

To be purchased from
York House, Kingsway, London W.C.2
423 Oxford Street, London W.1
13A Castle Street, Edinburgh 2
109 St. Mary Street, Cardiff
39 King Street, Manchester 2
50 Fairfax Street, Bristol 1
35 Smallbrook, Ringway, Birmingham 5
80 Chichester Street, Belfast 1
or through any bookseller

Printed in England

S.O. CODE No. 23-9013-16